

High Energy Cosmic Rays from the Decay of Gravitino Dark Matter

Koji Ishiwata^{(a)*}, Shigeki Matsumoto^{(b)†}, Takeo Moroi^{(a)‡}

^(a)*Department of Physics, Tohoku University, Sendai 980-8578, Japan*

^(b)*Department of Physics, University of Toyama, Toyama 930-8555, Japan*

Abstract

We study gamma ray and positron in high energy cosmic ray from the decay of the gravitino dark matter in the framework of supersymmetric model with R -parity violation. Even though R -parity is violated, the lifetime of the gravitino, which is assumed to be the lightest superparticle, can be longer than the present age of the universe if R -parity violating interactions are weak enough. In such a case, gravitino can be dark matter of the universe and its decay produces high energy cosmic rays. We calculate the fluxes of gamma ray and positron from the decay of the gravitino dark matter and discuss implications of such a scenario to present and future observations. In particular, we show that excesses of the fluxes of gamma ray and positron observed by EGRET and HEAT experiments, respectively, can be simultaneously explained as the cosmic rays from the decay of the gravitino dark matter.

*E-mail: ishiwata@tuhep.phys.tohoku.ac.jp

†E-mail: smatsu@sci.u-toyama.ac.jp

‡E-mail: moroi@tuhep.phys.tohoku.ac.jp

1 Introduction

In particle cosmology, origin of dark matter of the universe is one of the most important problems. Since there is no viable candidate for dark matter in the particle content of the standard model, new physics beyond the standard model is necessary to solve this problem. Supersymmetric model is a prominent candidate for the physics beyond the standard model; it not only introduces a viable candidate for dark matter, which is the lightest superparticle (LSP), but also solves other serious problems in particle physics, like naturalness problem of the electro-weak symmetry breaking.

In order to realize LSP dark matter scenario, conservation of R -parity is usually assumed. In [1], however, it has been pointed out that LSP dark matter scenario may be realized even with R -parity violation (RPV), if the LSP is the gravitino; even though gravitino LSP becomes unstable with RPV, its lifetime may be longer than the present age of the universe because the decay rate of the gravitino is suppressed by the Planck mass as well as by (small) RPV parameter. Such a scenario has a great advantage for the thermal leptogenesis scenario [2], as we will briefly discuss in the next section. Then, the primordial gravitino produced in the early universe can be a viable candidate for dark matter.

Even though the lifetime of the gravitino is much longer than the present age of the universe, a fraction of the gravitinos have decayed until today. Such a decay process becomes a source of high energy cosmic rays [1, 3]; the decay of the gravitino dark matter may produce high energy gamma ray and positron, which may be observed by present and future experiments.

In this paper, we investigate gamma-ray and positron fluxes from the decay of gravitino dark matter in supersymmetric model with RPV. We study the decay rate and branching ratios of the gravitino, taking account of all the relevant operators. Then, we calculate fluxes of gamma ray and positron from the decay of the gravitino dark matter, carefully taking account of the propagations of the cosmic rays. We discuss the implications of our results to the present and future observations of the high energy cosmic rays. Importantly, excesses of the gamma-ray and positron fluxes over the backgrounds are reported by Energetic Gamma Ray Experiment Telescope (EGRET) [4] and High Energy Antimatter Telescope (HEAT) [5] experiments, respectively. We will show that these excesses may be simultaneously explained by the scenario mentioned above.

The organization of this paper is as follows. In Section 2, we first summarize the cosmological scenario that we consider. In Section 3, we discuss the decay processes of the gravitino. In Section 4, formulae to calculate the cosmic-ray fluxes are given. The gamma-ray and positron fluxes from the decay of the gravitino dark matter are shown in Section 5; readers who are mainly interested in the results may directly go to this section. Section 6 is devoted to conclusions and discussion.

2 Cosmological Scenario

We first introduce the cosmological scenario that we consider. Although R -parity conservation is usually assumed in conventional studies of supersymmetric models, RPV has a favourable aspect in cosmology. In supersymmetric models, it is often the case that the thermal leptogenesis scenario [2], which is one of the most prominent scenarios to generate the present baryon asymmetry of the universe, is hardly realized since such a scenario requires relatively high reheating temperature after inflation, $T_R \gtrsim 10^9$ GeV [6, 7]. With such a high reheating temperature, gravitino overproduction problem arises for wide range of the gravitino mass as far as R -parity is conserved [8]. If the gravitino is unstable, gravitino produced after the reheating decays after the big-bang nucleosynthesis (BBN) starts and spoils the success of the BBN.^{#1} If the gravitino is stable, on the contrary, the primordial gravitino survives until today and contributes to the present energy density of the universe. Since the gravitino abundance increases as the gravitino mass becomes smaller, overclosure of the universe happens unless the gravitino mass is large enough [11]. With $T_R \gtrsim 10^9$ GeV, the above problems can be avoided only when (i) the gravitino is stable, and (ii) the gravitino mass is around 100 GeV. However, even in such a case, one has to worry about the decay of the lightest superparticle in the minimal supersymmetric standard model (MSSM) sector, which we call MSSM-LSP; with R -parity conservation, the MSSM-LSP, which is assumed to be the next-to-the-lightest superparticle (NLSP), decays only into gravitino and some standard-model particle(s). When $m_{3/2} \sim 100$ GeV, the lifetime of the MSSM-LSP becomes longer than 1 sec and relic MSSM-LSP decays after the BBN starts. When the MSSM-LSP is the neutralino or charged slepton, such decay processes spoil the success of the BBN, and hence it is difficult to realize the thermal leptogenesis scenario.

^{#1}However, $T_R \sim 10^9$ GeV may be also allowed when the gravitino mass is larger than $O(10$ TeV). Such a scenario may be realized in the class of anomaly-mediation model [9, 10].

If the R -parity is violated, the MSSM-LSP may decay via RPV interaction and its lifetime may become shorter than 1 sec. Then, $T_R \sim 10^9$ GeV is allowed. In such a case, gravitino is no longer stable and decays to standard-model particles. Even in such a case, however, the lifetime of the gravitino may be longer than the present age of the universe and hence the gravitino dark matter and thermal leptogenesis may be simultaneously realized [1].

Here, we consider the case where the gravitino is the LSP in the framework of the R -parity violated supersymmetric models. We assume that the present mass density of the gravitino is equal to the observed dark matter density so that the gravitino can play the role of dark matter. There are several possibilities of the origin of such a primordial gravitino: scattering processes of thermal particles [11] or the decay of scalar condensations [12]. We will not discuss in detail about the production mechanism of the primordial gravitino because the following arguments hold irrespective of the origin of the gravitino. In addition, we consider the case that the lifetime of the gravitino is much longer than the present age of the universe; the upper bounds on the size of RPV couplings will be discussed in the following section.

3 Framework and Decay Rates

In this section, we introduce the supersymmetric model that we consider. Then, we summarize the decay rates of the gravitino and the NLSP, which are important for our study.

3.1 Model

In this article, we concentrate on the case where the R -parity violating interactions originate from bi-linear terms of Higgs and lepton doublet. In the original basis, the R -parity violating interactions are assumed to be bi-linear terms in superpotential and supersymmetry (SUSY) breaking terms [13]. Without loss of generality, we can always eliminate the bi-linear R -parity violating terms from the superpotential by the redefinition of the Higgs and lepton-doublet multiplets. Then, the mixing terms between the Higgsino and lepton doublets are eliminated from the fermion mass matrix. In the following, we work in such a basis. Then, the relevant R -parity violating terms are only in the soft-SUSY breaking terms, which are given by

$$\mathcal{L}_{\text{RPV}} = B_i \tilde{L}_i H_u + m_{\tilde{L}_i H_d}^2 \tilde{L}_i H_d^* + \text{h.c.}, \quad (3.1)$$

where \tilde{L}_i is left-handed slepton doublet in i -th generation, while H_u and H_d are up- and down-type Higgs boson doublets, respectively. In the following, we study the phenomenological consequences of the R -parity violating terms given in Eq. (3.1).

With these R -parity violating terms, the vacuum expectation values (VEVs) of left-handed sneutrino fields $\tilde{\nu}_i$ are generated as

$$\langle \tilde{\nu}_i \rangle = \frac{B_i \sin \beta + m_{\tilde{L}_i H_d}^2 \cos \beta}{m_{\tilde{\nu}_i}^2} v, \quad (3.2)$$

where $v \simeq 174$ GeV is the VEV of standard-model-like Higgs boson, $\tan \beta = \langle H_u^0 \rangle / \langle H_d^0 \rangle$, and $m_{\tilde{\nu}_i}$ is the mass of $\tilde{\nu}_i$. The VEVs of the sneutrinos play important role in the following analysis. We parametrize the VEVs of the sneutrinos as

$$\kappa_i \equiv \frac{\langle \tilde{\nu}_i \rangle}{v}, \quad (3.3)$$

and consider the case that $\kappa_i \ll 1$.

One important constraint on the size of the R -parity violation is from the neutrino masses. Here, we assume that the neutrino masses are mainly from some other interaction, like the seesaw mechanism [14] or Dirac-type Yukawa interaction. However, the VEVs of sneutrinos also generate neutrino masses; assuming the Majorana-type masses for neutrinos, the ij component of the mass matrix receives the contribution of

$$[\Delta m_\nu]_{ij} = m_Z^2 \kappa_i \kappa_j \sum_\alpha \frac{|c_{\tilde{Z}\tilde{\chi}_\alpha^0}|^2}{m_{\tilde{\chi}_\alpha^0}}, \quad (3.4)$$

where m_Z is the Z -boson mass. In addition, Zino \tilde{Z} , which is the superpartner of the Z -boson, is related to the mass eigenstates of the neutralinos $\tilde{\chi}_\alpha^0$ (with mass $m_{\tilde{\chi}_\alpha^0}$) as

$$\tilde{Z} = \sum_\alpha c_{\tilde{Z}\tilde{\chi}_\alpha^0} \tilde{\chi}_\alpha^0. \quad (3.5)$$

(We also define the coefficients for photino and Higgsinos, $c_{\tilde{\gamma}\tilde{\chi}_\alpha^0}$, $c_{\tilde{H}_u^0\tilde{\chi}_\alpha^0}$, and $c_{\tilde{H}_d^0\tilde{\chi}_\alpha^0}$, by replacing $\tilde{Z} \rightarrow \tilde{\gamma}$, \tilde{H}_u^0 , and \tilde{H}_d^0 .) Assuming that the neutralino masses are close to the electro-weak scale so that the SUSY can be the solution to the fine-tuning problem of the electro-weak symmetry breaking, the correction to the neutrino mass matrix is estimated as

$$[\Delta m_\nu]_{ij} \sim 10^{-3} \text{ eV} \times \left(\frac{\kappa_i}{10^{-7}} \right) \left(\frac{\kappa_j}{10^{-7}} \right). \quad (3.6)$$

It indicates that the R -parity induced neutrino mass does not exceed experimental bound of observed neutrino mass when $\kappa_i \lesssim 10^{-7}$ is satisfied.

As we have mentioned, one of the important motivations to consider RPV is to relax the BBN constraints due to the decay of the MSSM-LSP. In a case that MSSM-LSP is Bino-like neutralino \tilde{B} , it decays in two-body processes, $\tilde{B} \rightarrow Z\nu_i$, Wl_i , and $h\nu_i$. The decay rates of each mode are given by^{#2}

$$\Gamma_{\tilde{B} \rightarrow Z\nu_i} = \frac{1}{128\pi} g_Z^2 \sin^2 \theta_W \kappa_i^2 m_{\tilde{B}} \left(1 - 3 \frac{m_Z^4}{m_{\tilde{B}}^4} + 2 \frac{m_Z^6}{m_{\tilde{B}}^6} \right), \quad (3.7)$$

$$\Gamma_{\tilde{B} \rightarrow Wl_i} = \frac{1}{64\pi} g_Z^2 \sin^2 \theta_W \kappa_i^2 m_{\tilde{B}} \left(1 - 3 \frac{m_W^4}{m_{\tilde{B}}^4} + 2 \frac{m_W^6}{m_{\tilde{B}}^6} \right), \quad (3.8)$$

$$\Gamma_{\tilde{B} \rightarrow h\nu_i} = \frac{1}{128\pi} g_Z^2 \sin^2 \theta_W \kappa_i^2 m_{\tilde{B}} \left(\frac{m_{\tilde{\nu}}^2}{m_{\tilde{\nu}}^2 - m_h^2} \right)^2 \left(1 - \frac{m_h^2}{m_{\tilde{B}}^2} \right)^2, \quad (3.9)$$

where $g_Z = \sqrt{g_1^2 + g_2^2}$ (with g_1 and g_2 being the gauge coupling constants of the $U(1)_Y$ and $SU(2)_L$ gauge groups, respectively), θ_W is the Weinberg angle, $m_{\tilde{B}}$ is Bino-like neutralino mass, and m_X ($X = Z, W, h$) is the mass of gauge or Higgs boson. Hence the lifetime is estimated as

$$\tau_{\tilde{B}} \simeq 0.07 \text{ sec} \times \left(\frac{\kappa}{10^{-11}} \right)^{-2} \left(\frac{m_{\tilde{B}}}{200 \text{ GeV}} \right)^2, \quad (3.10)$$

where

$$\kappa^2 \equiv \sum_i \kappa_i^2. \quad (3.11)$$

In another case that MSSM-LSP is right-handed stau $\tilde{\tau}_R$, it decays in the processes, $\tilde{\tau}_R \rightarrow \tau\nu_i$. In such a case, the decay rate is given by

$$\Gamma_{\tilde{\tau}_R} = \frac{1}{16\pi} g_Z^4 \sin^4 \theta_W \kappa^2 \left(\frac{v}{m_{\tilde{\chi}^0}} \right)^2 m_{\tilde{\tau}_R}, \quad (3.12)$$

where $m_{\tilde{\chi}^0}$ and $m_{\tilde{\tau}_R}$ masses of the lightest neutralino and stau, respectively, and the lifetime is estimated as

$$\tau_{\tilde{\tau}_R} \simeq 0.3 \text{ sec} \times \left(\frac{\kappa}{10^{-11}} \right)^{-2} \left(\frac{m_{\tilde{\chi}^0}}{300 \text{ GeV}} \right)^2 \left(\frac{m_{\tilde{\tau}_R}}{200 \text{ GeV}} \right)^{-1}. \quad (3.13)$$

Therefore, the lifetime of the MSSM-LSP, which is the NLSP in this case, becomes shorter than ~ 1 sec if typically $\kappa_i \gtrsim 10^{-11}$ is satisfied. Thus, combined with the

^{#2}Here, we consider the case that the lightest Higgs boson h is almost standard-model like, so that the Higgs mixing angle is given by the β parameter.

upper bound for κ_i from the neutrino mass, we focus on the parameter region:

$$10^{-11} \lesssim \kappa_i \lesssim 10^{-7}. \quad (3.14)$$

Before closing this subsection, we comment on the effects of tri-linear R -parity violating terms induced by the redefinition of the Higgs and lepton-doublet multiplets. With the redefinition of H_d and L_i to eliminate the bi-linear R -parity violating terms from the superpotential, tri-linear R -parity violating terms are induced. They are irrelevant for our following studies, but are constrained, in particular, from the wash-out of the baryon asymmetry of the universe.^{#3} Let us denote the tri-linear R -parity violating terms in the superpotential as

$$W_{\text{RPV}} = \lambda_{ijk} \hat{L}_k \hat{L}_i \hat{E}_j^c + \lambda'_{ijk} \hat{L}_k \hat{Q}_i \hat{D}_j^c, \quad (3.15)$$

where \hat{L}_i , and \hat{Q}_i are left-handed lepton, quark doublets, while \hat{E}_i^c and \hat{D}_i^c are right-handed lepton, down-quark singlets, respectively. (Here, “hat” is for superfield.) Then, in order not to wash out the baryon asymmetry of the universe, the coupling constants in the above superpotential are constrained as [15]

$$\lambda_{ijk}, \lambda'_{ijk} \lesssim 10^{-7}. \quad (3.16)$$

For example, if we assume that the size of R -parity violating terms are $O(\kappa_i)$ relative to the corresponding R -parity conserving ones (which are obtained by replacing \hat{H}_d with \hat{L}_i), and that the size of the SUSY breaking parameters are typically of the order of the electro-weak scale, then the above constraint is consistent with the one obtained from the neutrino mass.

3.2 Gravitino decay

In the case with RPV, gravitino LSP is no longer stable and decays to standard-model particles with a finite lifetime [16]. Here, we will take a closer look at the gravitino decay.

In the present scenario, gravitino mainly decays in the two-body decay processes shown in Fig. 1: $\psi_\mu \rightarrow \gamma\nu_i, Z\nu_i, Wl_i$, and $h\nu_i$. (Here and hereafter, ψ_μ denotes the

^{#3}In the present setup, baryon number is conserved, so the constraints from the nucleon decays are irrelevant.

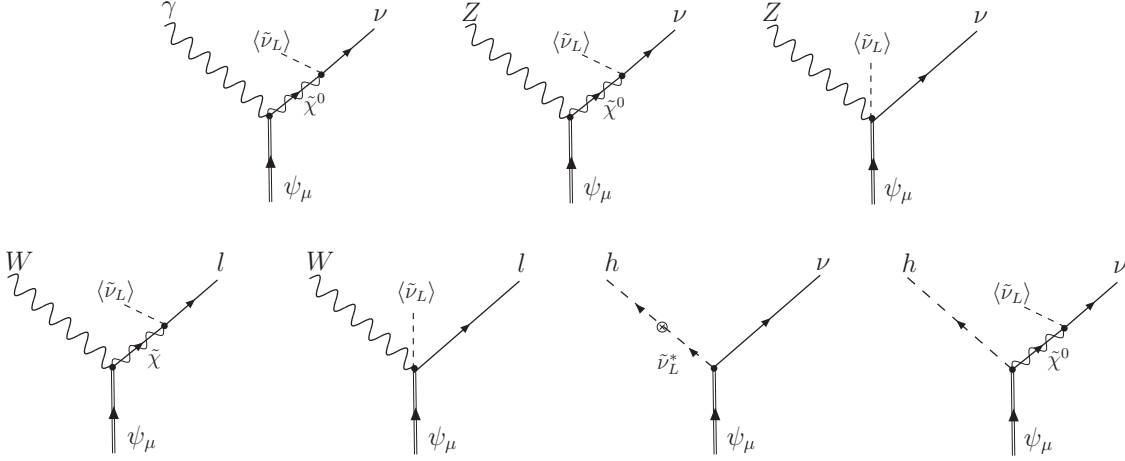


Figure 1: Diagrams of gravitino decay.

gravitino.) Decay widths of each process are given by^{#4}

$$\Gamma_{\psi_\mu \rightarrow \gamma \nu_i} = \frac{1}{128\pi} \frac{\kappa_i^2 m_{3/2}^3}{M_{\text{Pl}}^2} g_Z^2 \theta_{\tilde{\gamma}}^2, \quad (3.17)$$

$$\Gamma_{\psi_\mu \rightarrow Z \nu_i} = \frac{\beta_Z}{128\pi} \frac{\kappa_i^2 m_{3/2}^3}{M_{\text{Pl}}^2} \left[g_Z^2 \theta_{\tilde{Z}}^2 F(m_{3/2}, m_Z) + \frac{3v}{2m_{3/2}} g_Z^2 \theta_{\tilde{Z}} G(m_{3/2}, m_Z) + \frac{1}{3} \beta_Z H(m_{3/2}, m_Z) \right], \quad (3.18)$$

$$\Gamma_{\psi_\mu \rightarrow W l_i} = \frac{\beta_W}{64\pi} \frac{\kappa_i^2 m_{3/2}^3}{M_{\text{Pl}}^2} \left[g_W^2 \theta_{\tilde{W}}^2 F(m_{3/2}, m_W) + \frac{3v}{2m_{3/2}} g_W^2 \theta_{\tilde{W}} G(m_{3/2}, m_W) + \frac{1}{3} \beta_W H(m_{3/2}, m_W) \right] \quad (3.19)$$

$$\Gamma_{\psi \rightarrow h \nu_i} = \frac{\beta_h^4}{384\pi} \frac{\kappa_i^2 m_{3/2}^3}{M_{\text{Pl}}^2} \left(\frac{m_{\tilde{\nu}}^2}{m_{\tilde{\nu}}^2 - m_h^2} + m_Z \sin \beta \sum_{\alpha} \frac{c_{\tilde{H}_u^0 \tilde{\chi}_\alpha^0} c_{\tilde{Z} \tilde{\chi}_\alpha^0}^*}{m_{\tilde{\chi}_\alpha^0}} \right)^2, \quad (3.20)$$

where $M_{\text{Pl}} \simeq 2.4 \times 10^{18}$ GeV is the reduced Planck mass, $m_{3/2}$ is the gravitino mass,

$$\beta_X \equiv 1 - \frac{m_X^2}{m_{3/2}^2}, \quad (3.21)$$

^{#4}In [3], the coupling of the gravitino to the supercurrent of the slepton multiplet, which gives rise to the terms proportional to the functions G and H , was neglected. Consequently, the decay rates of the gravitino into $W^\pm l^\mp$ and $Z\nu$ are underestimated, resulting in enhanced branching ratio for the process $\psi_\mu \rightarrow \gamma\nu$.

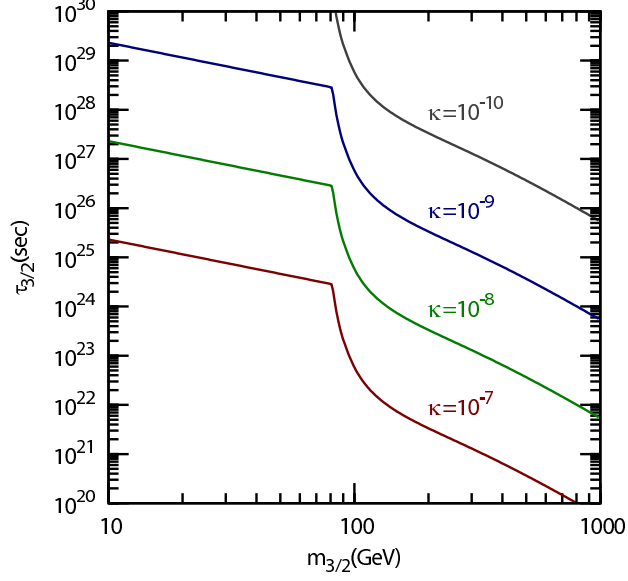


Figure 2: Lifetime of gravitino as a function of gravitino mass. Here, we take $\tan \beta = 10$, $m_h = 115$ GeV, $m_{\tilde{B}} = 1.5m_{3/2}$, $m_{\tilde{\nu}} = 2m_{3/2}$ under large Higgsino-mass limit, and assume GUT relation among gaugino masses.

and the functions F , G , and H are given by

$$F(m_{3/2}, m_X) = 1 - \frac{1}{3} \frac{m_X^2}{m_{3/2}^2} - \frac{1}{3} \frac{m_X^4}{m_{3/2}^4} - \frac{1}{3} \frac{m_X^6}{m_{3/2}^6}, \quad (3.22)$$

$$G(m_{3/2}, m_X) = 1 - \frac{1}{2} \frac{m_X^2}{m_{3/2}^2} - \frac{1}{2} \frac{m_X^4}{m_{3/2}^4}, \quad (3.23)$$

$$H(m_{3/2}, m_X) = 1 + 10 \frac{m_X^2}{m_{3/2}^2} + \frac{m_X^4}{m_{3/2}^4}. \quad (3.24)$$

In addition, we define

$$\theta_{\tilde{\gamma}} \equiv v \sum_{\alpha=1}^4 \frac{c_{\tilde{\gamma}\tilde{\chi}_\alpha^0} c_{\tilde{Z}\tilde{\chi}_\alpha^0}^*}{m_{\tilde{\chi}_\alpha^0}}, \quad (3.25)$$

$$\theta_{\tilde{Z}} \equiv v \sum_{\alpha=1}^4 \frac{c_{\tilde{Z}\tilde{\chi}_\alpha^0} c_{\tilde{Z}\tilde{\chi}_\alpha^0}^*}{m_{\tilde{\chi}_\alpha^0}}, \quad (3.26)$$

$$\theta_{\tilde{W}} \equiv \frac{1}{2} v \sum_{\alpha=1}^2 \frac{c_{\tilde{W}^+\tilde{\chi}_\alpha^+} c_{\tilde{W}^-\tilde{\chi}_\alpha^-} + \text{h.c.}}{m_{\tilde{\chi}_\alpha^\pm}}, \quad (3.27)$$

where $c_{\tilde{W}^\pm\tilde{\chi}_\alpha^\pm}$ is the elements of unitary matrices which diagonalize the mass matrix of charginos $\mathcal{M}_{\tilde{\chi}^\pm}$: $\tilde{W}^\pm = \sum_{\alpha=1}^2 c_{\tilde{W}^\pm\tilde{\chi}_\alpha^\pm} \tilde{\chi}_\alpha^\pm$ (i.e., $m_{\tilde{\chi}_\alpha^\pm} = \sum_{ij} c_{i\tilde{\chi}_\alpha^\mp} c_{j\tilde{\chi}_\alpha^\pm} [\mathcal{M}_{\tilde{\chi}^\pm}]_{ij}$).

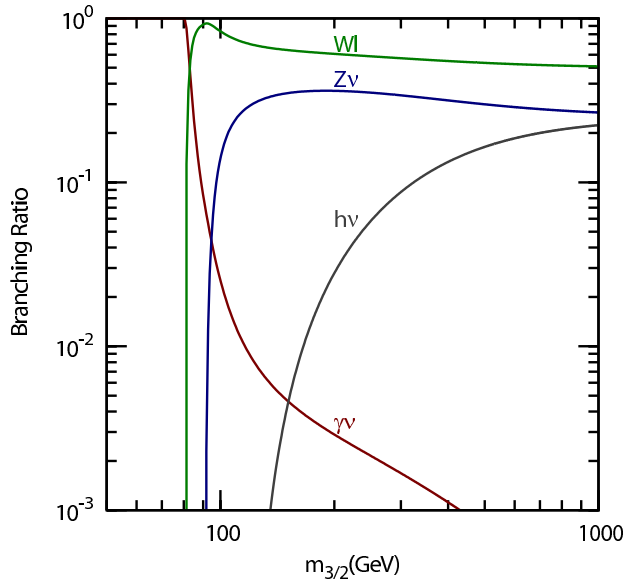


Figure 3: Branching ratio for each decay mode. Lines with the indices “ Wl ,” “ $Z\nu$,” “ $h\nu$ ” and “ $\gamma\nu$ ” show $Br(\psi_\mu \rightarrow W^+l^-) + Br(\psi_\mu \rightarrow W^-l^+)$, $Br(\psi_\mu \rightarrow Z\nu) + Br(\psi_\mu \rightarrow Z\bar{\nu})$, $Br(\psi_\mu \rightarrow h\nu) + Br(\psi_\mu \rightarrow h\bar{\nu})$, and $Br(\psi_\mu \rightarrow \gamma\nu) + Br(\psi_\mu \rightarrow \gamma\bar{\nu})$, respectively. (Summation over the generation index is implicit.) Here, we take the MSSM parameters used in Fig. 2

Lifetime of gravitino is determined by these two-body decay processes:

$$\tau_{3/2}^{-1} = \Gamma_{3/2} = 2 \sum_{i=1}^3 [\Gamma_{\psi_\mu \rightarrow \gamma\nu_i} + \Gamma_{\psi_\mu \rightarrow Z\nu_i} + \Gamma_{\psi_\mu \rightarrow Wl_i} + \Gamma_{\psi \rightarrow h\nu_i}], \quad (3.28)$$

where the factor of 2 is for CP-conjugated final states. In Fig. 2, we plot $\tau_{3/2}$ as a function of $m_{3/2}$ in the large Higgsino-mass limit. Here, we take $\tan\beta = 10$, $m_h = 115$ GeV, $m_{\tilde{\nu}} = 2m_{3/2}$, $m_{\tilde{B}} = 1.5m_{3/2}$, and grand unified theory (GUT) relation among the gaugino masses are assumed. One can see that $\tau_{3/2}$ is much longer than the age of the universe ($\simeq 4.3 \times 10^{17}$ sec) for weak-scale gravitino mass when $\kappa \lesssim 10^{-7}$. Thus, in such a parameter region, most of gravitinos produced in the early universe survive until the present epoch.

Even though the lifetime of the gravitino is long enough to realize the gravitino dark matter scenario, it may be possible to observe the decay of gravitino dark matter at present epoch. In particular, high energy photons and positrons are emitted in the decay processes as well as in the following cascade decay processes. To see this, in Fig. 3, we show branching ratio of each decay mode for $\tan\beta = 10$ in the large Higgsino mass limit. (Notice that the branching ratios are independent of κ_i .)

When $m_{3/2} \lesssim 80$ GeV, the decay mode $\psi_\mu \rightarrow \gamma\nu$ dominates in total decay rate, because the decay processes with the emission of the weak or Higgs boson are kinematically blocked. On the contrary, once the gravitino becomes heavier than the weak bosons, the branching ratio for the process $\psi_\mu \rightarrow \gamma\nu$ is suppressed. This behavior can be understood from the fact that the θ -parameters defined in Eqs. (3.25) – (3.27), in particular, $\theta_{\tilde{\gamma}}$, is suppressed when the neutralino and chargino masses become much larger than the electro-weak scale.

This fact has important implication in the study of the scenario using cosmic rays. When the gravitino is lighter than ~ 100 GeV or so, line spectrum of the gamma ray may be a striking signal. With larger gravitino mass, on the contrary, it becomes difficult to observe the gamma-ray line spectrum. Even in that case, however, significant amount of gamma rays with the energy of $O(1 - 100$ GeV) are emitted in the cascade decays of Z , W , and h bosons. Therefore, the continuous high energy gamma ray could be used as another characteristic signal. In addition to the gamma ray, high energy positrons are also emitted, which is another interesting signal from the decay of gravitino dark matter.

4 Cosmic-Ray Fluxes: Formulae

As we have discussed in the previous section, energetic gamma and positron are produced if gravitino decays via R -parity violating interactions. If gravitino is dark matter of the universe, such decay products can be a source of high energy cosmic rays. In order to discuss how well the scenario is tested by the use of cosmic ray, it is necessary to formulate the calculation of the cosmic-ray fluxes from the decay of gravitino. In this section, we show how we calculate the gamma-ray and positron fluxes from the gravitino decay.

4.1 Gamma ray from the gravitino decay

The total flux of the gamma ray from the decay of dark matter (i.e., gravitino) is calculated by the sum of two contributions:

$$\left[\frac{dJ_\gamma}{dE} \right]_{\text{DM}} = \left[\frac{dJ_\gamma}{dE} \right]_{\text{cosmo}} + \left[\frac{dJ_\gamma}{dE} \right]_{\text{halo}}, \quad (4.1)$$

where the first and second terms in the right-hand side are fluxes of gamma ray from cosmological distance and that from the Milky Way halo, respectively. We discuss

these contributions separately.

The flux of the gamma ray from cosmological distance is estimated as

$$\left[E^2 \frac{dJ_\gamma}{dE} \right]_{\text{cosmo}} = \frac{E^2}{m_{3/2} \tau_{3/2}} \int_E^\infty dE' G_\gamma(E, E') \frac{dN_\gamma(E')}{dE'}. \quad (4.2)$$

Here, the propagation function of gamma ray is given by

$$G_\gamma(E, E') = \frac{c \rho_c \Omega_{3/2}}{4\pi H_0 \Omega_M} \frac{1}{E} \left(\frac{E}{E'} \right)^{3/2} \frac{1}{\sqrt{1 + \Omega_\Lambda / \Omega_M (E/E')^3}}, \quad (4.3)$$

where c is the speed of light, H_0 is present Hubble expansion rate, ρ_c is critical density, and $\Omega_{3/2} \simeq 0.105h^{-2}$, $\Omega_M \simeq 0.127h^{-2}$, $\Omega_\Lambda \simeq 0.76h^{-2}$ (with $h \simeq 0.73$) are density parameters of gravitino dark matter, total matter, and dark energy, respectively [17]. In addition, dN_γ/dE is the energy spectrum of gamma ray from the decay of single gravitino, which can be given by the sum of contributions from relevant decay modes:

$$\begin{aligned} \frac{dN_\gamma}{dE} = & \frac{2}{\Gamma_{3/2}} \sum_{i=1}^3 \left(\Gamma_{\psi_\mu \rightarrow \gamma \nu_i} \left[\frac{dN_\gamma}{dE} \right]_{\gamma \nu_i} + \Gamma_{\psi_\mu \rightarrow Z \nu_i} \left[\frac{dN_\gamma}{dE} \right]_{Z \nu_i} \right. \\ & \left. + \Gamma_{\psi_\mu \rightarrow W l_i} \left[\frac{dN_\gamma}{dE} \right]_{W l_i} + \Gamma_{\psi_\mu \rightarrow h \nu_i} \left[\frac{dN_\gamma}{dE} \right]_{h \nu_i} \right). \end{aligned} \quad (4.4)$$

Here, $[dN_\gamma/dE]_{\dots}$ are energy distributions for each decay modes. Notice that the dN_γ/dE is determined once the SUSY parameters are fixed, irrespective of the cosmological scenario. We calculate dN_γ/dE by using PYTHIA package [18].

The flux of the gamma ray from the Milky Way Galaxy halo is obtained as [19]

$$\left[E^2 \frac{dJ_\gamma}{dE} \right]_{\text{halo}} = \frac{E^2}{m_{3/2} \tau_{3/2}} \frac{1}{4\pi} \frac{dN_\gamma}{dE} \left\langle \int_{\text{l.o.s.}} \rho_{3/2}(\vec{l}) d\vec{l} \right\rangle_{\text{dir}}, \quad (4.5)$$

where $\rho_{3/2}$ is the energy density of the gravitino in the Milky Way halo. In Eq. (4.5), the integration should be understood to extend over the line of sight (l.o.s.). Thus, the integration has an angular dependence on the direction of observation. Here, $[E^2 dJ_\gamma/dE]_{\text{halo}}$ is given by averaging over the direction, which is denoted as $\langle \dots \rangle_{\text{dir}}$. In the EGRET observation, the signal from the Galactic disc is excluded in order to avoid the noise. In order to compare our results with the EGRET results, we also exclude the region within $\pm 10^\circ$ around the Galactic disk in averaging over the direction.

In order to perform the line-of-sight integration, the profile of $\rho_{3/2}$, namely dark matter mass density profile ρ_{halo} , should be given. For our numerical analysis, we

adopt Navarro-Frenk-White (NFW) density profile [20]:

$$\rho_{\text{halo}}(r) = \frac{\rho_h}{r/r_c(1 + r/r_c)^2}, \quad (4.6)$$

where r is the distance from the Galactic center, $\rho_h \simeq 0.33 \text{ GeV cm}^{-3}$, and $r_c \simeq 20 \text{ kpc}$. We have checked that the dependence on the dark matter profile is negligible because, in the calculation of the gamma-ray flux, we exclude the region around the Galactic disc as we have mentioned.

4.2 Positron from the gravitino decay

Next, we discuss cosmic-ray positron from the gravitino decay. If we consider energetic positron propagating in galaxy, its trajectory is twisted because of magnetic field. With the expected strength of the magnetic field, scale of gyro-radius of the trajectory is much smaller than the size of the galaxy. Furthermore, the magnetic field in the galaxy is entangled. Because of these, propagation of the positron in the galaxy is expected to be well approximated as a random walk.

We use a diffusion model for the propagation of positron, in which random walk is described by the following diffusion equation [21, 22]:

$$\frac{\partial f_{e^+}(E, \vec{x})}{\partial t} = K(E)\nabla^2 f_{e^+}(E, \vec{x}) + \frac{\partial}{\partial E} [b(E)f_{e^+}(E, \vec{x})] + Q(E, \vec{x}), \quad (4.7)$$

where $f_{e^+}(E, \vec{x})$ is the number density of positrons per unit energy (with E being the energy of positron), $K(E)$ is the diffusion coefficient, $b(E)$ is the energy loss rate, and $Q(E, \vec{x})$ is the positron source term. As we mentioned above, diffusion of injected positron is caused by the entangled magnetic field in the galaxy. On the other hand, the energy loss of the positron is via Thomson and inverse Compton scatterings with Cosmic Microwave Background and infrared gamma ray from stars or Synchrotron radiation under the magnetic field. The functions $K(E)$ and $b(E)$ can be determined so that the cosmic-ray Boron to Carbon ratio and sub-Fe to Fe ratio are reproduced. In our analysis, we use those given in [21]:

$$K(E) = 3.3 \times 10^{27} \times \left[1.39 + \left(\frac{E}{1 \text{ GeV}} \right)^{0.6} \right] \text{ cm}^2 \text{ sec}^{-1}, \quad (4.8)$$

$$b(E) = 10^{-16} \times \left(\frac{E}{1 \text{ GeV}} \right)^2 \text{ GeVsec}^{-1}. \quad (4.9)$$

Since the magnitude of the energy loss rate indicates that positron loses its energy in the flight of less than a few kpc, the positron flux from outside of our Milky

Way Galaxy halo is negligible. Thus, in the following discussion, we focus on the contribution of the positron flux from the Milky Way Galaxy. In addition, the positron source term is given by the use of the positron injection rate and dark matter distribution in the Milky Way Galaxy halo as^{#5}

$$Q(E, \vec{x}) = \frac{\rho_{\text{halo}}(\vec{x})}{m_{3/2}} \frac{1}{\tau_{3/2}} \frac{dN_{e^+}}{dE}, \quad (4.10)$$

where dN_{e^+}/dE is energy distribution of positron from the decay of single gravitino. The explicit expression is given as

$$\begin{aligned} \frac{dN_{e^+}}{dE} = & \frac{1}{\Gamma_{3/2}} \sum_{i=1}^3 \left(2\Gamma_{\psi_\mu \rightarrow Z\nu_i} \left[\frac{dN_{e^+}}{dE} \right]_{Z\nu_i} + \Gamma_{\psi_\mu \rightarrow Wl_i} \left[\frac{dN_{e^+}}{dE} \right]_{W^-l_i^+} \right. \\ & \left. + \Gamma_{\psi_\mu \rightarrow Wl_i} \left[\frac{dN_{e^+}}{dE} \right]_{W^+l_i^-} + 2\Gamma_{\psi_\mu \rightarrow h\nu_i} \left[\frac{dN_{e^+}}{dE} \right]_{h\nu_i} \right), \end{aligned} \quad (4.11)$$

where $[dN_{e^+}/dE]_{\dots}$ is energy distribution for each decay mode. We calculate the energy distributions by the use of PYTHIA package. For density distribution, we adopt the same profile as the previous section, namely NFW profile defined in Eq. (4.6).

We solve the diffusion equation in finite diffusion zone with boundary condition. Since the observed cosmic-ray positrons are considered to be in equilibrium, we impose stability condition $\partial f(E, \vec{x})/\partial t = 0$, and also free escape condition $f(E, \vec{x}) = 0$ at the boundary. The diffusion zone is usually assumed as cylinder characterized with half-height L and radius R . Since positrons lose their energy after the flight of a few kpc or less, the positron flux does not strongly depend on the choice of the diffusion zone. In our analysis, we take $L = 4$ kpc and $R = 20$ kpc.

Positron flux from the decay of gravitino dark matter is given by

$$[\Phi_{e^+}(E)]_{\text{DM}} \equiv \frac{dJ_{e^+}}{dE} = \frac{c}{4\pi} f(E, \vec{R}_\odot), \quad (4.12)$$

where \vec{R}_\odot is the location of the solar system. This flux does not correspond exactly to the one observed on the top of the atmosphere. The flux is modified due to interaction with solar wind and magneto-sphere. However, the modulation effect is not important when the energy of a positron is above 10 GeV. Furthermore, the effect is highly suppressed in the positron fraction, which is defined by the ratio of the positron flux to the sum of positron and electron fluxes, i.e., $\Phi_{e^+}/(\Phi_{e^+} + \Phi_{e^-})$.

^{#5}The uncertainty on the positron flux from the effect of inhomogeneity in the local dark matter distribution is negligible [23], which is quite contrast to the traditional case of dark matter annihilation.

4.3 Backgrounds

In order to discuss high energy gamma ray and positron as signals from the decay of dark-matter gravitino, it is important to understand those cosmic rays from other sources. (We call them backgrounds.)

Cosmic gamma rays have various origins. As we have mentioned, the cosmic gamma rays can be divided into two parts by their origins; Galactic and extragalactic parts. Some part of the Galactic origins, such as scattering processes (i.e., inverse Compton scattering and bremsstrahlung) and pion decay, are known as probable sources of cosmic gamma rays. However, other Galactic origins, as well as the extragalactic ones, have not been well understood. In the study of the gamma ray from the gravitino decay, it is important to understand the behavior of the unidentified cosmic gamma ray (UCGR) from various origins.^{#6} However, theoretical calculation of such components of the cosmic gamma ray is difficult, so we adopt more phenomenological approach to extract the UCGR not originating from the gravitino decay.

Currently, the cosmic gamma ray flux has been measured by EGRET, and various analysis have been performed to extract the UCGR from the EGRET data. The first intensive work was done in [4], in which it is concluded that the UCGR follows a power law as $E^2 dJ_\gamma/dE = 1.37 \times 10^{-6} (E/1 \text{ GeV})^{-0.1} (\text{cm}^2 \text{ str sec})^{-1} \text{ GeV}$. Generally, however, there is a difficulty in removing the contribution from the known scattering or decay processes in the Milky Way Galaxy since the analysis depends on the Galactic model. Recently, with an improved analysis in the estimation of the Galactic contribution [30, 31], it has been pointed out that the UCGR spectrum follows a power-law in the energy range $E \lesssim 1 \text{ GeV}$. However, for $E \gtrsim 1 \text{ GeV}$, a deviation from the power-law behavior is reported. As we will see, the effect of the gravitino decay on the cosmic gamma ray becomes important for the energy range of $E \gtrsim 0.1 - 1 \text{ GeV}$. Thus, in our analysis, we assume that the UCGR in the lower energy

^{#6}The UCGR may have various origins. Examples in astrophysics are contributions from galaxy clusters [24], energetic particles in the shock waves associated with large-scale cosmological structure formation [25], distant gamma-ray burst events, baryon-antibaryon annihilation [26]. In addition, if we consider physics beyond the standard model, spectrum of UCGR may be affected by, for example, the evaporation of primordial black holes [27], the annihilation of weakly interacting massive particles (WIMPs) [28, 21, 22], or extragalactic IR and optical photon spectra [29]. In our analysis, we only consider the decay of the gravitino as a particle-physics source of the UCGR, and do not consider other possibilities.

range is only from astrophysical origins (although many of them have not yet been well understood). In addition, we also assume that the spectrum of UCGR from astrophysical origins follows a power law, and hence its behavior can be extracted from the data in the sub-GeV region. Since the gamma ray from the gravitino becomes important above the energy of 0.1 – 1 GeV, we use the observed data in the range of 0.05 GeV < E < 0.15 GeV to determine the background flux. Assuming the power-law behavior, we obtain the best-fit UCGR flux as

$$\left[E^2 \frac{dJ_\gamma}{dE} \right]_{\text{BG}} \simeq 5.18 \times 10^{-7} (\text{cm}^2 \text{ sec str})^{-1} \text{ GeV} \times \left(\frac{E}{\text{GeV}} \right)^{-0.449}. \quad (4.13)$$

We use this spectrum as the background in the following analysis. Then, the total gamma-ray spectrum is given by

$$\left[\frac{dJ_\gamma}{dE} \right]_{\text{tot}} = \left[\frac{dJ_\gamma}{dE} \right]_{\text{DM}} + \left[\frac{dJ_\gamma}{dE} \right]_{\text{BG}}. \quad (4.14)$$

Next, let us consider the background positron (and electron). Cosmic rays mainly consist of nuclei, electrons, and positrons. Nuclei are the dominant component of the cosmic rays and pouring to the earth after it has drifted by interaction with interstellar matters in our Galaxy. As a consequence, secondary cosmic-ray electrons and positrons are produced. On the theoretical side, many simulations of cosmic-ray electron and positron have been done by the use of cosmic-ray propagation model [30]. In our study, we adopt the following cosmic-ray electron and positron from astrophysical processes [21]:

$$[\Phi_{e^-}]_{\text{prim}} = \frac{0.16 E_{\text{GeV}}^{-1.1}}{1 + 11 E_{\text{GeV}}^{0.9} + 3.2 E_{\text{GeV}}^{2.15}} (\text{GeV cm}^2 \text{ sec str})^{-1}, \quad (4.15)$$

$$[\Phi_{e^-}]_{\text{sec}} = \frac{0.70 E_{\text{GeV}}^{0.7}}{1 + 110 E_{\text{GeV}}^{1.5} + 600 E_{\text{GeV}}^{2.9} + 580 E_{\text{GeV}}^{4.2}} (\text{GeV cm}^2 \text{ sec str})^{-1}, \quad (4.16)$$

$$[\Phi_{e^+}]_{\text{sec}} = \frac{4.5 E_{\text{GeV}}^{0.7}}{1 + 650 E_{\text{GeV}}^{2.3} + 1500 E_{\text{GeV}}^{4.2}} (\text{GeV cm}^2 \text{ sec str})^{-1}, \quad (4.17)$$

where E_{GeV} is the energy of electron or positron in units of GeV. We note here that concerning the backgrounds, the secondary electron accounts for about 10 % of the total electron flux while the positron flux is dominated by the secondary one.

With these backgrounds, the total fluxes of the electron and positron are obtained as

$$[\Phi_{e^+}]_{\text{tot}} = [\Phi_{e^+}]_{\text{DM}} + [\Phi_{e^+}]_{\text{sec}}, \quad (4.18)$$

$$[\Phi_{e^-}]_{\text{tot}} = [\Phi_{e^-}]_{\text{DM}} + [\Phi_{e^-}]_{\text{prim}} + [\Phi_{e^-}]_{\text{sec}}. \quad (4.19)$$

Importantly, the above background in cosmic-ray positron flux well agrees with HEAT observation in the energy range $E \lesssim 10$ GeV. However, for $E \gtrsim 10$ GeV, an excess of the positron flux is seen in the HEAT data [5]. In the following section, we show that such an excess may be due to the decay of gravitino.^{#7}

5 Numerical Results

5.1 Cosmic rays from the gravitino decay

Now we are at the position to present our numerical results. In this subsection, we show fluxes of cosmic-ray gamma and positron from the gravitino decay to discuss their behaviors.

First, we discuss the gamma-ray flux. The flux for $m_{3/2} = 150$ GeV is shown on the left in Fig. 4. (Here, the lifetime of $\tau_{3/2} = 10^{26}$ sec is used.) We found that the dependence of the gamma-ray flux on the flavor of the primary lepton is negligible. (Here and hereafter, for the calculation of the gamma-ray flux, we assume that the gravitino mainly decays into third-generation leptons and gauge or Higgs bosons.) In calculating the gamma-ray flux, we adopt the energy resolution of 15 %, following EGRET [4]. In the figures, we also show the contributions of individual decay modes. (In this case, the contribution of the decay mode into $h\nu$ is very small.)

As one can see, continuous spectrum is obtained from the decay modes into weak boson (or Higgs boson) and lepton, while a relatively steep peak is also obtained at $E = \frac{1}{2}m_{3/2}$ due to the monochromatic gamma emission via $\psi_\mu \rightarrow \gamma\nu$. With larger gravitino mass, $Br(\psi_\mu \rightarrow \gamma\nu)$ is suppressed, and hence the peak at $E = \frac{1}{2}m_{3/2}$ becomes less significant. Thus, when the gravitino mass becomes much larger than the masses of weak bosons, it will become difficult to find such a line spectrum.

The positron fraction is shown on the right in Fig. 4 for the cases where the gravitino dominantly decays into first, second, and third generation leptons. Since the energy of positron becomes smaller during the propagation in the Galaxy, the positron spectrum has the upper end point at $\sim \frac{1}{2}m_{3/2}$. In particular, when the gravitino can directly decay into positron, the end point becomes a steep edge; such an edge can be a striking signal of the decaying dark matter if observed. Even in other cases, the positron spectrum has a peak just below the upper end point. This may also provide an interesting signal in the observed positron flux.

^{#7}For other possibilities, see [21, 22].

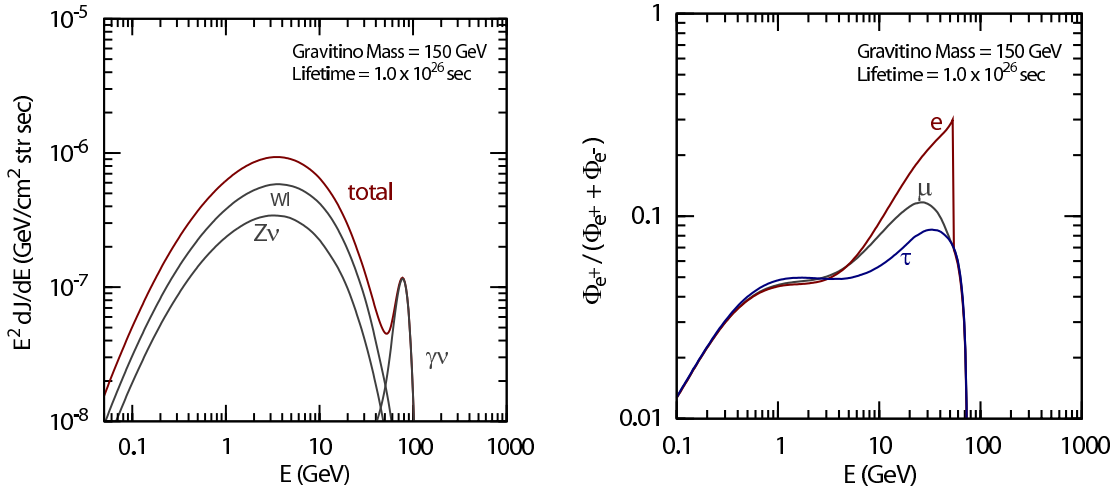


Figure 4: Left: Gamma-ray flux from gravitino decay $[E^2 dJ_\gamma/dE]_{\text{DM}}$ (“total”). Lines with “ $\gamma\nu$,” “ $Z\nu$,” and “ Wl ” are contributions from each decay mode. Right: Positron fraction $[\Phi_{e^+}]_{\text{DM}}/([\Phi_{e^+}]_{\text{tot}} + [\Phi_{e^-}]_{\text{tot}})$. Lines with “ e ,” “ μ ,” and “ τ ” show the results for the case that the gravitino mainly decays to first, second, and third generation leptons, respectively. For both of the figures, we take $m_{3/2} = 150$ GeV, $\tau_{3/2} = 1.0 \times 10^{26}$ sec, and the MSSM parameters used in Fig. 2.

So far, we have shown results only for the case of $\tau_{3/2} = 10^{26}$ sec. Fluxes with other values of the lifetime can be easily obtained from the above results since the cosmic-ray fluxes from the gravitino decay is inversely proportional to $\tau_{3/2}$. One important point is that, when $\tau_{3/2} = O(10^{26}$ sec), both the gamma-ray and positron fluxes from the gravitino decay become comparable to the background fluxes discussed in the previous section for $E \sim 1 - 100$ GeV. Thus, with such a lifetime, we may be able to see the signal of the decay of gravitino dark matter in the spectrum of cosmic rays. The following subsections are devoted to the discussion of such an issue.

5.2 Implications to present observations

As discussed in the previous section, some anomalies are indicated both in the gamma-ray spectrum observed by EGRET and the positron fraction observed by HEAT. In this subsection, we show that these anomalies may be simultaneously explained by a single scenario, the gravitino dark matter scenario with RPV.

In Fig. 5, we show the total gamma-ray flux and the positron fraction for $m_{3/2} = 150$ GeV and $\tau_{3/2} = 2.1 \times 10^{26}$ sec. (We have used the best fit value of $\tau_{3/2}$ for the EGRET data.) Here, we consider simple cases where the gravitino decays only into

one of the three lepton flavors; only one of the $\langle \tilde{\nu}_i \rangle$ ($i = 1 - 3$) is non-vanishing while the others are set to be zero. (For gamma ray, the total flux is independent of generation indices as we have mentioned in the previous subsection.) With the lifetime adopted, the gamma-ray flux and the positron fraction both significantly deviate from the background. In gamma-ray flux (Fig. 5, left), one can see that the continuous spectrum originating from the processes $\psi_\mu \rightarrow Wl$ and $Z\nu$ gives a good agreement with EGRET data for $E \sim 1 - 10\text{GeV}$. In the positron fraction (Fig. 5, right), the results indicate that clear signal can be seen in the energy region $E \gtrsim 10$ GeV over the background for all the three cases. In the same figure, we also show the observational data of EGRET or HEAT. As one can see, agreements between the theoretical predictions and observations are improved both for EGRET and HEAT.

Results for other values of the gravitino mass (and lifetime) are shown in Figs. 6 and 7. We can see that the suggested anomalies in the gamma-ray and positron fluxes may be explained in a wide range of the gravitino mass.

In order to see the preferred parameter region in the light of EGRET result, we calculate the χ^2 variable as a function of $m_{3/2}$ and $\tau_{3/2}$:

$$\chi^2 = \sum_{i=1}^N \frac{(x_{\text{th},i} - x_{\text{obs},i})^2}{\sigma_{\text{obs},i}^2}, \quad (5.1)$$

where $x_{\text{th},i}$ is the theoretically calculated flux in i -th bin, which is calculated with Eq. (4.14), $x_{\text{obs},i}$ is the observed flux, and $\sigma_{\text{obs},i}$ is the error of $x_{\text{obs},i}$. In addition, N is number of bins; $N = 10$ for EGRET. In Fig. 8, we show the region with $\chi^2 < 18.3$ on the $m_{3/2}$ vs. $\tau_{3/2}$ plane, which is 95 % C.L. allowed region. As one can see, the present scenario could well explain the EGRET anomaly in a wide parameter region, $10^{26} \text{ sec} \lesssim \tau_{3/2} \lesssim 10^{27} \text{ sec}$ and $m_{3/2} \gtrsim 90 \text{ GeV}$. From Fig. 2, it can be seen that $10^{-10} \lesssim \kappa_i \lesssim 10^{-8}$ is favored. In Fig. 8, we also show the parameter region which is consistent with the HEAT data ($N = 9$) at 95 % C.L. (i.e., $\chi^2 < 16.9$).

As one can see, the present scenario can simultaneously explain the observed gamma and positron fluxes.

5.3 Future prospects

In the previous subsection, we have shown that the gamma-ray and positron fluxes from decaying gravitinos can successfully explain the results of the past observations. As we have seen, however, the energy ranges of the past observations are limited up to $O(10 \text{ GeV})$ although the signal from the gravitino decay may significantly affect

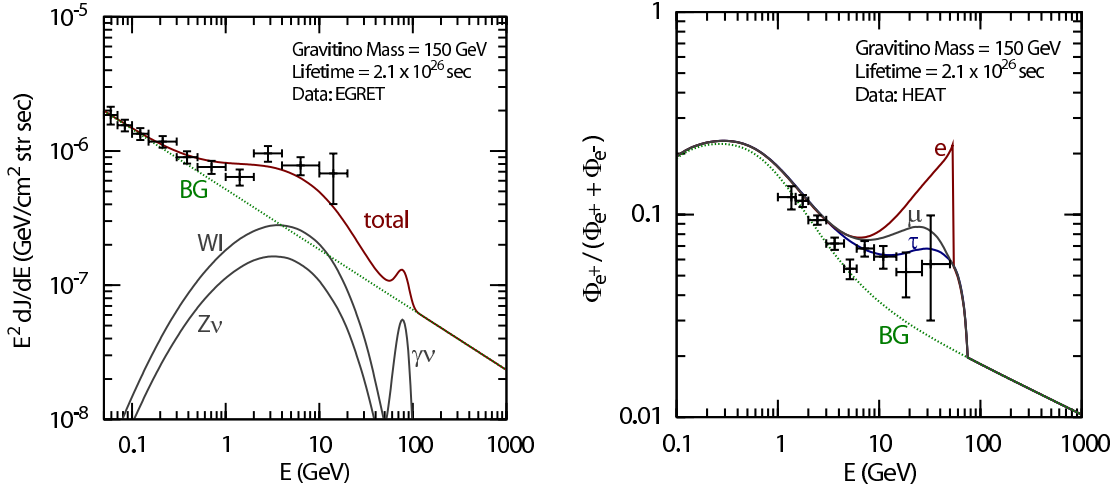


Figure 5: Gamma-ray flux (left figure) and positron fraction (right figure). Here, we take $m_{3/2} = 150$ GeV, $\tau_{3/2} = 2.1 \times 10^{26}$ sec, and MSSM parameters as Fig. 2.

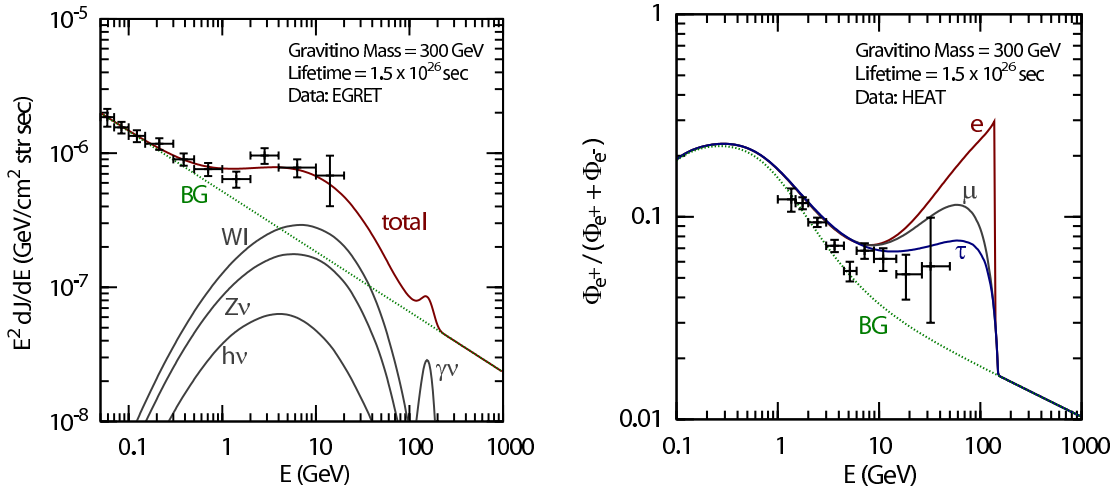


Figure 6: Same as Fig. 5, except for $m_{3/2} = 300$ GeV and $\tau_{3/2} = 1.5 \times 10^{26}$ sec.

the cosmic-ray spectra up to the energy of $O(100$ GeV). In addition, it is also true that the uncertainties of the cosmic-ray spectra observed by the past observations are relatively large at the energy range of $E \sim O(10$ GeV). Thus, it is desirable to test the scenario of gravitino dark matter with RPV with better observations.

Fortunately, in the near future, new observations of cosmic rays, GLAST and PAMELA, are expected to provide results of new measurements of the cosmic-ray fluxes. These experiments are designed to detect cosmic rays with energy up to a few hundreds GeV. Thus, they will give us better test of the scenario. Since GLAST (PAMELA) has better energy range and resolution than EGRET (HEAT) in the measurement of gamma-ray (positron) flux, they should confirm the anomalies if

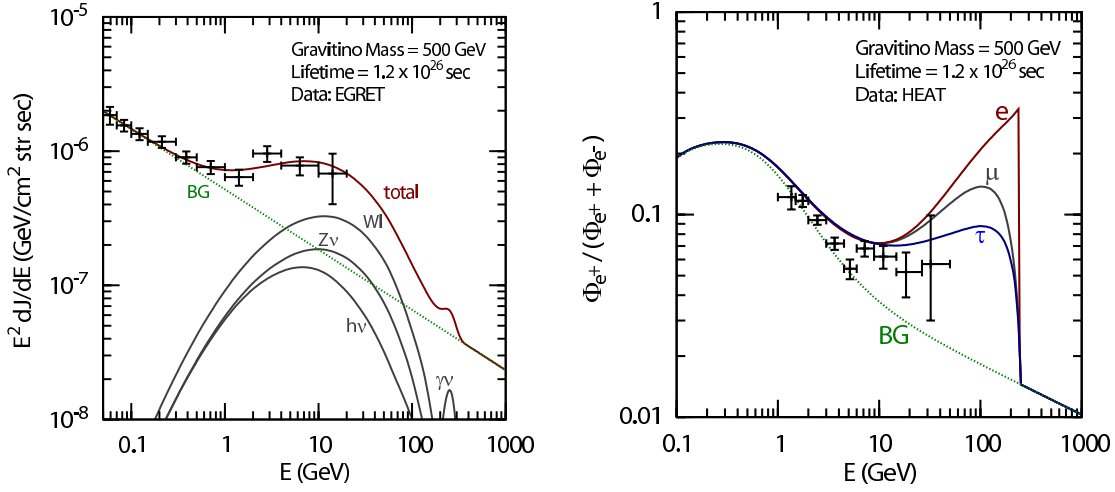


Figure 7: Same as Fig. 5, except for $m_{3/2} = 500$ GeV and $\tau_{3/2} = 1.2 \times 10^{26}$ sec.

they really exist.

Even if the fluxes of the cosmic rays are smaller than the best-fit value of those observed by EGRET and HEAT, we still have a chance to see signals from the decay of dark-matter gravitino. To see expected constraints on the parameter space, we calculate the expectation value of the χ^2 variable defined as

$$\langle \chi^2 \rangle = \left\langle \sum_{i=1}^N \frac{(N_{\text{th},i} - N_{\text{BG},i})^2}{\sigma_{\text{BG},i}^2} \right\rangle, \quad (5.2)$$

where N is the number of bins. We use 50 bins to estimate the expected sensitivities of GLAST and PAMELA. With the use of GLAST and PAMELA instrument parameters [32, 33, 34], we define i -th bin as $E_{\gamma/e^+,i}^{(\min)} \leq E_{\gamma/e^+,i} < E_{\gamma/e^+,i}^{(\max)}$, where

$$E_{\gamma,i}^{(\min)} = 0.02 \text{ GeV} \times \left(\frac{300 \text{ GeV}}{0.02 \text{ GeV}} \right)^{\frac{i-1}{50}}, \quad (5.3)$$

$$E_{e^+,i}^{(\min)} = 0.05 \text{ GeV} \times \left(\frac{270 \text{ GeV}}{0.05 \text{ GeV}} \right)^{\frac{i-1}{50}}, \quad (5.4)$$

and $E_{\gamma/e^+,i}^{(\max)} = E_{\gamma/e^+,i+1}^{(\min)}$. In addition, $N_{\text{th},i}$ is the number of theoretically calculated events in i -th bin, which is the expected number of events in GLAST or PAMELA experiment. Notice that $N_{\text{th},i}$ is calculated by using Eq. (4.14) or Eq. (4.18). Furthermore, $N_{\text{BG},i}$ is the number of background events. Here, we assume that the number of background events will be well understood in the future observations by using the data in low-energy range; in our following study, we use Eqs. (4.13) and

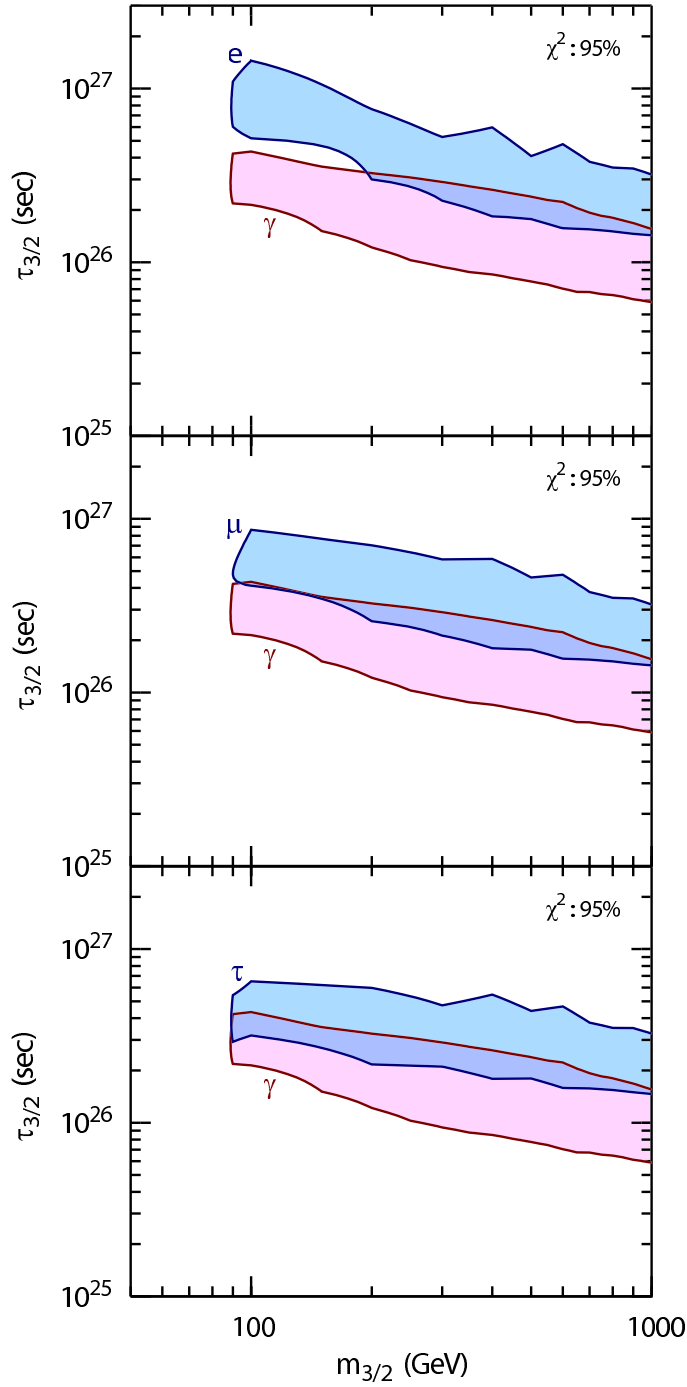


Figure 8: 95% C.L. allowed regions on $m_{3/2}$ vs. $\tau_{3/2}$ plane; the shaded regions are the allowed regions. The region with “ γ ” is for the EGRET data, while the region with “ e ” (“ μ ,” “ τ ”) is for HEAT data for the case where the gravitino decays into first- (second-, third-) generation lepton.

(4.17). Then, we obtain

$$N_{\text{th},i} = \left[\frac{dJ_\gamma(E_{\gamma,i})}{dE} \right]_{\text{tot}} \Delta E_{\gamma,i} TS, \quad (5.5)$$

$$N_{\text{BG},i} = \left[\frac{dJ_\gamma(E_{\gamma,i})}{dE} \right]_{\text{BG}} \Delta E_{\gamma,i} TS, \quad (5.6)$$

for gamma-ray flux, and

$$N_{\text{th},i} = [\Phi_{e^+}(E_{e^+,i})]_{\text{tot}} \Delta E_{e^+,i} TS, \quad (5.7)$$

$$N_{\text{BG},i} = [\Phi_{e^+}(E_{e^+,i})]_{\text{sec}} \Delta E_{e^+,i} TS, \quad (5.8)$$

for cosmic-ray positron flux. Here, T and S are exposure time and acceptance, respectively, and $\sigma_{\text{BG},i}$ is the error of the number of backgrounds, which we take $\sigma_{\text{BG},i} = \sqrt{N_{\text{BG},i}}$ assuming that the error is dominated by statistics. In our analysis, we take $TS = 10^{10}$ and 10^8 cm² sec str for GLAST and PAMELA, respectively. In addition, $\Delta E_{\gamma/e^+,i} = E_{\gamma/e^+,i}^{(\text{max})} - E_{\gamma/e^+,i}^{(\text{min})}$ is the width of the i -th bin.

Expected constraints on the $m_{3/2}$ vs. $\tau_{3/2}$ plane is shown in Fig. 9. For positron flux, we consider the case that the primary lepton emitted by the gravitino decay is τ or ν_τ . In Fig. 9, we show contours of $\langle \chi^2 \rangle = 67.5$, corresponding to 95 % level of detectability. From the figure, one can see that the signal from decaying gravitino will be observed in both observations in wide range of the parameter space.

6 Conclusions and Discussion

In this paper, we have discussed the high energy cosmic rays from the decay of gravitino dark matter in R -parity violated supersymmetric model. Here, we have considered the case that the gravitino is the LSP, and that RPV originates from the $L_i H_u$ -type operators. In such a model, the gravitino dominantly decays into a gauge boson (W^\pm , Z , or γ) and a lepton with extremely long lifetime. In particular, if RPV interactions are weak enough, the lifetime of the gravitino becomes much longer than the present age of the universe. Consequently, if the right amount of the gravitino is produced in the early universe, gravitino can be dark matter even if the R -parity is not conserved. In addition, in such a scenario, the MSSM-LSP, which is assumed to be the NLSP, can decay with a lifetime shorter than ~ 1 sec via RPV operators. Then, the serious effects on the light element abundances by the decay of the NLSP, which gives one of the most stringent constraint on the scenario of gravitino dark matter, can be avoided.

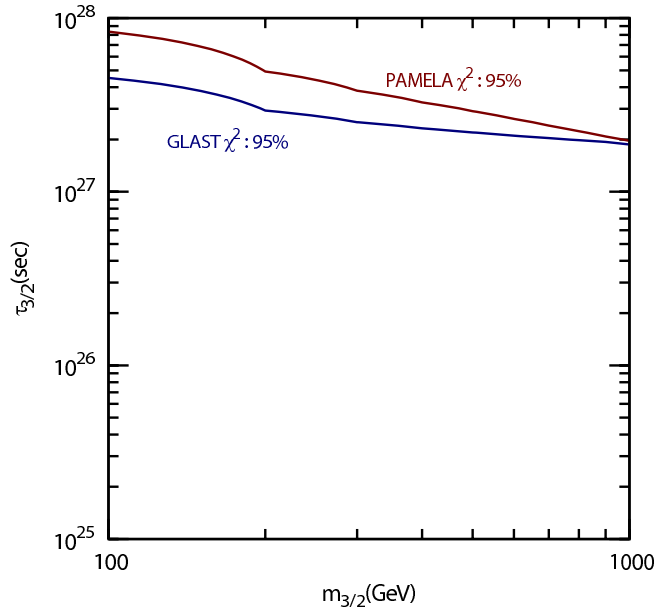


Figure 9: Contour plot of $\langle \chi^2 \rangle$ on $m_{3/2}$ vs. $\tau_{3/2}$ plane for 95% probability to detect gamma-ray/positron signal from gravitino decay in GLAST/PAMELA.

We have studied the gamma-ray and positron fluxes from the decay of the gravitino dark matter. In our analysis, we have calculated the decay rate and branching ratios of the gravitino, taking account of all the relevant operators. Then, the energy spectrum of the primary decay products (i.e., gauge bosons, leptons, and partons) are calculated. Decay and hadronization processes of those primary particles have been treated by using PYTHIA package to accurately calculate the primary fluxes of gamma ray and positron by the decay of gravitino. Then, by solving the propagation equations, we have obtained the fluxes of gamma ray and positron in the cosmic ray.

One of our important results is that the anomalies observed by the EGRET and HEAT experiments can be simultaneously explained in this scenario if the lifetime of the gravitino is $O(10^{26}$ sec). This conclusion holds for a wide range of the gravitino mass; as far as $m_{3/2}$ is larger than ~ 80 GeV so that the gravitino can decay into weak boson(s), such a scenario works. In addition, with PAMELA and GLAST, more accurate test of the scenario will become possible; they will cover the parameter region of $\tau_{3/2} \lesssim 10^{27-28}$ sec.

We comment here that, in the present scenario, the MSSM-LSP decays via RPV interactions, which may affect the LHC phenomenology. If the EGRET and HEAT anomalies are due to the decay of the gravitino dark matter, the lifetime of the

MSSM-LSP is estimated to be $O(10^{-5} \text{ sec})$. This fact may have an impact on the LHC experiment. The typical decay length of the MSSM-LSP is $O(10^3 \text{ m})$, which is much longer than the size of the detector. Thus, most of the MSSM-LSPs produced at the LHC experiment escape from the detector before the decay. If the lightest neutralino is the LSP, the collider signatures are the same as the conventional signatures with the neutralino LSP. However, in the present scenario, the MSSM-LSP may be charged (or even colored). In such a case, we will observe a heavy charged particle as high p_T track at the LHC. In addition, 0.1 – 1 % of the produced MSSM-LSP may decay in the detector, resulting in isolated vertices from the interaction point. These are very exotic signals which are not expected in the conventional model of supersymmetry.

So far, we have considered the case where the gravitino is dark matter. However, with other candidates for dark matter, it may be possible to simultaneously explain the excesses of the gamma-ray and positron fluxes observed by EGRET and HEAT experiments. In particular, if dark matter decays mainly into the weak bosons with the lifetime of $\sim 10^{26} \text{ sec}$, this can be the case. One of the examples may be the lightest neutralino. With RPV, the lightest neutralino decays even if it is the LSP; with the RPV operator given in Eq. (3.1), for example, the lifetime of the neutralino LSP becomes $\sim 10^{26} \text{ sec}$ when $\kappa \sim 10^{-25}$, assuming that the lightest neutralino is Bino-like and that the mass of the lightest neutralino is $\sim 100 \text{ GeV}$.

Note added: While finalizing this paper, we found [35] which also studies high energy cosmic rays from the decay of the gravitino dark matter. In the study of the gravitino decay in [35], effects of the coupling of the gravitino to the supercurrent of the slepton multiplet have not been taken into account.

Acknowledgments: This work was supported in part by Research Fellowships of the Japan Society for the Promotion of Science for Young Scientists (K.I.), and by the Grant-in-Aid for Scientific Research from the Ministry of Education, Science, Sports, and Culture of Japan, No. 19540255 (T.M.).

References

- [1] W. Buchmuller, L. Covi, K. Hamaguchi, A. Ibarra and T. Yanagida, JHEP **0703**, 037 (2007).
- [2] M. Fukugita and T. Yanagida, Phys. Lett. B **174**, 45 (1986).

- [3] A. Ibarra and D. Tran, Phys. Rev. Lett. **100**, 061301 (2008).
- [4] P. Sreekumar *et al.* [EGRET Collaboration], Astrophys. J. **494**, 523 (1998).
- [5] S. W. Barwick *et al.* [HEAT Collaboration], Astrophys. J. **482**, L191 (1997).
- [6] W. Buchmuller, P. Di Bari and M. Plumacher, Annals Phys. **315**, 305 (2005).
- [7] G. F. Giudice, A. Notari, M. Raidal, A. Riotto and A. Strumia, Nucl. Phys. B **685**, 89 (2004).
- [8] For the recent study, see, for example, M. Kawasaki, K. Kohri, T. Moroi and A. Yotsuyanagi, arXiv:0804.3745 [hep-ph].
- [9] G. F. Giudice, M. A. Luty, H. Murayama and R. Rattazzi, JHEP **9812** (1998) 027.
- [10] L. Randall and R. Sundrum, Nucl. Phys. B **557** (1999) 79.
- [11] T. Moroi, H. Murayama and M. Yamaguchi, Phys. Lett. B **303**, 289 (1993).
- [12] M. Endo, K. Hamaguchi and F. Takahashi, Phys. Rev. Lett. **96**, 211301 (2006); S. Nakamura and M. Yamaguchi, Phys. Lett. B **638**, 389 (2006); M. Dine, R. Kitano, A. Morisse and Y. Shirman, Phys. Rev. D **73**, 123518 (2006); M. Endo, K. Hamaguchi and F. Takahashi, Phys. Rev. D **74**, 023531 (2006); M. Kawasaki, F. Takahashi and T. T. Yanagida, Phys. Lett. B **638**, 8 (2006); Phys. Rev. D **74**, 043519 (2006); M. Endo, F. Takahashi and T. T. Yanagida, Phys. Rev. D **76**, 083509 (2007); Phys. Lett. B **658**, 236 (2008).
- [13] S. Roy and B. Mukhopadhyaya, Phys. Rev. D **55**, 7020 (1997); F. Takayama and M. Yamaguchi, Phys. Lett. B **476**, 116 (2000); M. Hirsch, M. A. Diaz, W. Porod, J. C. Romao and J. W. F. Valle, Phys. Rev. D **62**, 113008 (2000) [Erratum-ibid. D **65**, 119901 (2002)]; A. Abada, S. Davidson and M. Losada, Phys. Rev. D **65**, 075010 (2002); E. J. Chun, D. W. Jung and J. D. Park, Phys. Lett. B **557**, 233 (2003).
- [14] T. Yanagida, in “Proceedings of the Workshop on Unified Theory and Baryon Number of the Universe,” eds. O. Sawada and A. Sugamoto (KEK, 1979) p.95; M. Gell-Mann, P. Ramond and R. Slansky, in “Supergravity,” eds. P. van Nieuwenhuizen and D. Freedman (North Holland, 1979); S. L. Glashow, in “Proceedings of the Cargèse Summer Institute on Quarks and Leptons,” (Plenum, 1980) p707.

- [15] B. A. Campbell, S. Davidson, J. R. Ellis and K. A. Olive, Phys. Lett. B **256**, 484 (1991); W. Fischler, G. F. Giudice, R. G. Leigh and S. Paban, Phys. Lett. B **258**, 45 (1991); H. K. Dreiner and G. G. Ross, Nucl. Phys. B **410**, 188 (1993).
- [16] F. Takayama and M. Yamaguchi, Phys. Lett. B **485**, 388 (2000).
- [17] D. N. Spergel *et al.*, Astrophys. J. Suppl. **148**, 175 (2003).
- [18] T. Sjostrand, S. Mrenna and P. Skands, JHEP **0605**, 026 (2006)
- [19] T. Asaka, J. Hashiba, M. Kawasaki and T. Yanagida, Phys. Rev. D **58**, 023507 (1998); G. Bertone, W. Buchmuller, L. Covi and A. Ibarra, JCAP **0711**, 003 (2007).
- [20] J. F. Navarro, C. S. Frenk and S. D. M. White, Astrophys. J. **490**, 493 (1997).
- [21] E. A. Baltz and J. Edsjo, Phys. Rev. D **59**, 023511 (1999).
- [22] J. Hisano, S. Matsumoto, O. Saito and M. Senami, Phys. Rev. D **73**, 055004 (2006); M. Asano, S. Matsumoto, N. Okada and Y. Okada, Phys. Rev. D **75**, 063506 (2007)
- [23] J. Silk and A. Stebbins, Astrophys. J. **411** (1993) 439; L. Bergstrom, J. Edsjo and P. Gondolo, Phys. Rev. D **59** (1999) 043506.
- [24] T. A. Ensslin, P. L. Biermann, P. P. Kronberg and X. P. Wu, Astrophys. J. **477**, 560 (1997);
- [25] A. Loeb and E. Waxman, Nature **405**, 156 (2000); F. Miniati, Mon. Not. Roy. Astron. Soc. **337**, 199 (2002);
- [26] Y. T. Gao, F. W. Stecker, M. Gleiser and D. B. Cline, Astrophys. J. **361**, L37 (1990); A. Dolgov and J. Silk, Phys. Rev. D **47**, 4244 (1993).
- [27] S. W. Hawking, Nature **248**, 30 (1974); K. Maki, T. Mitsui and S. Orito, Phys. Rev. Lett. **76**, 3474 (1996).
- [28] G. Jungman, M. Kamionkowski and K. Griest, Phys. Rept. **267**, 195 (1996).
- [29] F. W. Stecker, Astropart. Phys. **11**, 83 (1999).
- [30] I. V. Moskalenko and A. W. Strong, Astrophys. J. **493**, 694 (1998); A. W. Strong and I. V. Moskalenko, Astrophys. J. **509**, 212 (1998); A. W. Strong, I. V. Moskalenko and O. Reimer, Astrophys. J. **537**, 763 (2000) [Erratum-ibid. **541**, 1109 (2000)];
- [31] A. W. Strong, I. V. Moskalenko and O. Reimer, Astrophys. J. **613**, 956 (2004).

- [32] N. Gehrels and P. Michelson, *Astropart. Phys.* **11**, 277 (1999).
- [33] M. Boezio *et al.*, *Nucl. Phys. Proc. Suppl.* **134**, 39 (2004).
- [34] D. Hooper and J. Silk, *Phys. Rev. D* **71**, 083503 (2005).
- [35] A. Ibarra and D. Tran, arXiv:0804.4596 [astro-ph].